The Journal of Nutrition
Nutrient Physiology, Metabolism, and Nutrient-Nutrient Interactions

Mitochondrial Fatty Acid β-Oxidation Inhibition Promotes Glucose Utilization and Protein Deposition through Energy Homeostasis Remodeling in Fish

Ling-Yu Li,[1] Jia-Min Li,[1,2] Li-Jun Ning,[3] Dong-Liang Lu,[1] Yuan Luo,[1] Qiang Ma,[1] Samwel Mchele Limbu,[1,4] Dong-Liang Li,[1] Li-Qiao Chen,[1] Irfan J Lodhi,[5] Pascal Degrace,[6] Mei-Ling Zhang,[1] and Zhen-Yu Du[1]

[1]LANEH, School of Life Sciences, East China Normal University, Shanghai, China; [2]Fisheries College, Ocean University of China, Qingdao, China; [3]College of Marine Sciences, South China Agricultural University, Guangzhou, China; [4]Department of Aquatic Sciences and Fisheries Technology, University of Dar es Salaam, Dar es Salaam, Tanzania; [5]Division of Endocrinology, Metabolism & Lipid Research, Washington University School of Medicine, Saint Louis, MO, USA; and [6]Team Pathophysiology of Dyslipidemia, INSERM UMR1231 Lipids, Nutrition, Cancer, Université de Bourgogne Franche-Comté, Dijon, France

ABSTRACT

Background: Fish cannot use carbohydrate efficiently and instead utilize protein for energy supply, thus limiting dietary protein storage. Protein deposition is dependent on protein turnover balance, which correlates tightly with cellular energy homeostasis. Mitochondrial fatty acid β-oxidation (FAO) plays a crucial role in energy metabolism. However, the effect of remodeled energy homeostasis caused by inhibited mitochondrial FAO on protein deposition in fish has not been intensively studied.

Objectives: This study aimed to identify the regulatory role of mitochondrial FAO in energy homeostasis maintenance and protein deposition by studying lipid, glucose, and protein metabolism in fish.

Methods: Carnitine-depleted male Nile tilapia (initial weight: 4.29 ± 0.12 g; 3 mo old) were established by feeding them with mildronate diets (1000 mg/kg/d) for 6 wk. Zebrafish deficient in the carnitine palmitoyltransferase 1b gene (*cpt1b*) were produced by using CRISPR/Cas9 gene-editing technology, and their males (154 ± 3.52 mg; 3 mo old) were used for experiments. Normal Nile tilapia and wildtype zebrafish were used as controls. We assessed nutrient metabolism and energy homeostasis–related biochemical and molecular parameters, and performed ^{14}C-labeled nutrient tracking and transcriptomic analyses.

Results: The mitochondrial FAO decreased by 33.1–88.9% (liver) and 55.6–68.8% (muscle) in carnitine-depleted Nile tilapia and *cpt1b*-deficient zebrafish compared with their controls ($P < 0.05$). Notably, glucose oxidation and muscle protein deposition increased by 20.5–24.4% and 6.40–8.54%, respectively, in the 2 fish models compared with their corresponding controls ($P < 0.05$). Accordingly, the adenosine 5′-monophosphate–activated protein kinase/protein kinase B–mechanistic target of rapamycin (AMPK/AKT-mTOR) signaling was significantly activated in the 2 fish models with inhibited mitochondrial FAO ($P < 0.05$).

Conclusions: These data show that inhibited mitochondrial FAO in fish induces energy homeostasis remodeling and enhances glucose utilization and protein deposition. Therefore, fish with inhibited mitochondrial FAO could have high potential to utilize carbohydrate. Our results demonstrate a potentially new approach for increasing protein deposition through energy homeostasis regulation in cultured animals. *J Nutr* 2020;00:1–14.

Keywords: energy homeostasis, fatty acid β-oxidation, fish, glucose utilization, insulin sensitivity, protein synthesis

Introduction

Animal protein is the predominant source of protein for humans around the world (1), thus humans require optimal animal production with maximum protein deposition. From a cellular metabolism point of view, the deposition of protein in cells depends on protein synthesis and breakdown (2, 3), which correlate with energy homeostasis. Protein deposition mainly depends on a dynamic balance among protein, carbohydrate, and lipid metabolism (3, 4). In cells, energy metabolites such as amino acids (AAs), glucose, fatty acids (FAs), pyruvate, acetyl CoA, triglycerides (TGs), and lactate are in a dynamic balance, which is regulated by metabolic interactions among major nutrients (4, 5). Accumulating evidence from mammalian studies shows that loss of mitochondrial fatty acid β-oxidation

Manuscript received April 12, 2020. Initial review completed May 2, 2020. Revision accepted June 11, 2020.
First published online 0, 2020; doi: https://doi.org/10.1093/jn/nxaa187.

(FAO) activates adenosine 5′-monophosphate–activated protein kinase (AMPK), consequently increasing glucose utilization via activation of the insulin signaling protein kinase B (AKT) pathway (6–9) and AA catabolism (6). In contrast, inhibition of glucose oxidation by pharmacological or genetic approaches increases FAO for fuels (10, 11). However, the correlation between protein deposition and energy homeostasis has not been well addressed in most organisms.

In most mammals, protein turnover in muscle is commonly constant in adults (2, 12). Different from mammals, fish often exhibit a sustained growth, with body size and muscle mass increasing until death or senescence occurs (13). In addition, as poikilothermic organisms, fish have lower energy consumption and higher feed conversion efficiency compared with most terrestrial animals (14). Accordingly, the amount of tissue protein deposited per unit of dietary energy intake is much higher in fish than in omnivorous birds and mammals (15). Currently, fish and other seafood products rank as the third protein provider after cereals and milk, accounting for 6.5% of total protein supply and 16.4% of total animal protein consumed globally (1). Therefore, increasing protein deposition in fish is widely viewed as an opportunity to meet the rising demand for animal-derived protein in the world.

However, unlike mammals, which use carbohydrate as the main energy source, fish preferentially use protein (16). Therefore, fish require higher dietary protein levels compared with terrestrial animals, and a large portion of the dietary protein is broken down for energy provision and consequently unavailable for protein supply to humans (14). In classic fish nutrition theory, fish have a poor ability to utilize dietary carbohydrates (16, 17). Therefore, high dietary carbohydrate often causes metabolic disturbances in many fish species, such as severe fat accumulation and reduced growth and feed efficiency (18, 19). Considering the increasing cost and limited supply of aquafeed protein sources such as fishmeal, approaches to ensure higher glucose/carbohydrate utilization and protein deposition are top research priorities for fish physiologists. Recently, our fish studies have provided clues that changes in FAO can affect body glycogen content and expression of glycolysis-related genes and mechanistic target of rapamycin (mTOR) (18, 20–22). However, to the best of our knowledge, a systematic investigation of energy homeostasis after mitochondrial FAO inhibition has never been performed in fish.

This study was supported by National Key Research and Development Project (2018YFD0900400) and the National Natural Science Fund (31830102 and 31772859).
Author disclosures: The authors report no conflicts of interest.
Supplemental Methods, Supplemental Tables 1–6, Supplemental Figures 1–10, and Supplemental Figure Caption are available from the "Supplementary data" link in the online posting of the article and from the same link in the online table of contents at https://academic.oup.com/jn/.
Address correspondence to Z-YD (e-mail: zydu@bio.ecnu.edu.cn).
Abbreviations used: AA, amino acid; AKT, protein kinase B; ALT, alanine transaminase; AMPK, adenosine 5′-monophosphate–activated protein kinase; *asns*, asparagine synthetase; AST, aspartate transaminase; *atf4*, activating transcription factor 4; *cpt1b*$^{-/-}$, carnitine palmitoyltransferase 1b knockout; Ctrl, control; cytb, cytochrome b; DEG, differentially expressed gene; DMEM, Dulbecco modified Eagle medium; dpf, days postfertilization; FA, fatty acid; FAO, fatty acid β-oxidation; *gcn2*, general control nonderepressible 2; GTT, glucose tolerance test; HK, hexokinase; IR, insulin receptor; MD, mildronate; MDA, malondialdehyde; MFI, mesenteric fat index; MK, MK-2206 2HCl (AKT pathway inhibitor); mpf, months postfertilization; mTOR, mechanistic target of rapamycin; OCR, oxygen consumption rate; PA, palmitic acid; p-AKT, phosphorylation of protein kinase B; PK, pyruvate kinase; p-S6, phosphorylation of S6 ribosomal protein; qRT-PCR, quantitative real-time PCR; Rap, rapamycin; S6, S6 ribosomal protein; TAA, total amino acids; TG, triglyceride; wt, wildtype; β-HB, β-hydroxybutyrate.

Here, we characterized the crucial role of mitochondrial FAO in regulating fish energy metabolism. We hypothesized that inhibited mitochondrial FAO promotes protein deposition through remodeling energy homeostasis. Thus, we established 2 fish models with inhibited mitochondrial FAO: carnitine-depleted Nile tilapia (*Oreochromis niloticus*) and carnitine-palmitoyltransferase 1b knockout (*cpt1b*$^{-/-}$) zebrafish (*Danio rerio*). Nile tilapia and zebrafish are both warm-water omnivorous teleosts, and their entire genomes are available (21, 22); they have been widely used in metabolic research (21, 23, 24). In the present study, we used the Nile tilapia and zebrafish with inhibited mitochondrial FAO to identify the regulatory roles of mitochondrial FAO in nutrient metabolism and the related molecular mechanisms involved in remodeled energy homeostasis in fish.

Methods

Animal ethics

Animal studies were conducted in compliance with the Guide for the Care and Use of Laboratory Animals in China. All animal procedures were approved by the Committee on Ethics of Animal Experiments of East China Normal University (approval number F20140101).

Animal sources

All male Nile tilapia juveniles were purchased from the Shanghai Ocean University. Before the formal studies, the fish were acclimated at 28°C in a semicircular aquaculture system with a 14 h/10 h light/dark cycle, and fed a commercial diet (Tilapia Compound Feed 1055, Tongwei Co. Ltd) containing 40% protein and 7% lipid for 2 wk. Six-month-old adult zebrafish (0.3–0.4 g) were purchased from the Chinese National Zebrafish Resource Center. The zebrafish obtained were used as broodstock for establishment of mutants. The zebrafish were maintained at 28°C in a recirculating aquaculture system equipped with a mechanical filter and an aquarium heater in a 14 h/10 h light/dark cycle. The zebrafish were fed twice a day with freshly hatched brine shrimp eggs.

Carnitine-depleted Nile tilapia establishment

The carnitine-depleted Nile tilapia were established based on previous fish and mammalian studies (22, 25, 26). The male Nile tilapia were administered mildronate (MD) (Chengdu Micxy Chemical Co. Ltd) at a dose of 1000 mg/kg/d. To achieve this, 180 visually healthy Nile tilapia with comparable initial mean weight (4.29 ± 0.12 g) were selected and randomly distributed into 2 groups; control (Ctrl) and MD (3 replicates per group, 30 fish per replicate). The fish were hand-fed twice daily with either a Ctrl diet or an MD diet for 6 wk (**Supplemental Table 1**). For more details on dietary preparation and feeding strategy, see **Supplemental Methods**. At the end of the feeding trial, all fish were fasted for 12 h. Nine fish from each group were killed by anesthetizing them with 20 mg/L tricaine methanesulfonate. The liver and abdominal adipose tissue from these fish were collected and weighed for calculation of organ indices such as hepatosomatic index and mesenteric fat index (MFI). Serum, liver, and muscle samples were also collected from each dead fish. The samples were frozen immediately in liquid nitrogen, followed by storage at −80°C for further physiological analysis. Another 6 fish from each group were killed after anesthetization and stored at −80°C for body composition analysis.

Establishment of *cpt1b* mutant zebrafish and fish maintenance

The *cpt1b* mutant zebrafish were established by using CRISPR/Cas9 gene-editing technology as described in our previous study (27). For details on *cpt1b* knockout (*cpt1b*$^{-/-}$) zebrafish establishment, see Supplemental Methods. The resulting F3 zebrafish *cpt1b*$^{-/-}$ and wildtype (wt) larvae were analyzed for *cpt1b* mRNA expression and CPT1b protein abundance [1 mo postfertilization (mpf)], swimming

activity [5 d postfertilization (dpf)], Nile red staining (15 dpf) (28), and oxygen consumption rate (OCR, 15 dpf) by using a Strathkelvin Instruments 782 Oxygen Meter system. We further fed the 3 mpf-old male *cpt1b*$^{-/-}$ mutants (154 ± 3.52 mg) and wt fish (162 ± 2.87 mg) a commercial diet (Shengsuo) containing 40% protein and 8% lipid for 4 wk. At the end of the feeding trial, all fish were fasted for 12 h, and the whole body, liver, muscle, and blood samples were collected and frozen immediately for further analysis.

Metabolic profiling of mitochondrial FAO–inhibited models

Six to 8 Nile tilapia samples from Ctrl and MD treatments, and 18 zebrafish samples from wt and *cpt1b*$^{-/-}$ mutants were collected for determination of metabolic and physiological parameters. The total protein content was determined by the Kjeldahl method after acid digestion using a 2300 Kjeltec Analyzer Unit (FOSS Tecator) (28). The total lipid content was measured by using the chloroform/methanol (2:1 v/v) method (29). The nonessential fatty acids (R & D Systems) and insulin (Millipore) were measured by using specific ELISA kits. The contents of β-hydroxybutyrate (β-HB), TGs, malondialdehyde (MDA), glucose, total AAs (TAA), lactate, pyruvate, and glycogen, and the activities of aspartate transaminase (AST), alanine transaminase (ALT), hexokinase (HK), and pyruvate kinase (PK) were assessed by using specific commercial kits (Jiancheng Biotech Co) based on manufacturer's instructions. The hydrolysis of muscle protein was performed by using the conventional acidic hydrolysis method as described previously (30). The AA composition in muscle was assessed from Nile tilapia of Ctrl and MD treatments and from zebrafish from wt and *cpt1b*$^{-/-}$ mutants by using a Hitachi L-8900 Automatic Amino Acid Analyzer. For more details on AA composition analysis, see Supplemental Methods.

Carnitine concentration determination

The liver and muscle samples from 6 Nile tilapia of Ctrl and MD treatments were collected for determination of free carnitine concentrations. The details of sample preparation and LC-MS measurement were as described previously (20). For more details on carnitine concentration determination, see Supplemental Methods.

Acetyl-CoA concentration measurement

The acetyl-CoA concentrations in liver and muscle of Nile tilapia from Ctrl and MD treatments and of zebrafish from wt and *cpt1b*$^{-/-}$ mutants were determined by using HPLC as described previously (31). The HPLC run was completed in 15 min without any additional time for column re-equilibration between the HPLC runs. For more details on acetyl-CoA concentration measurement, see Supplemental Methods.

FAO assay

The liver and muscle samples from 6 Nile tilapia of Ctrl and MD treatments, and from 9 zebrafish of wt and *cpt1b*$^{-/-}$ mutants were collected and homogenized for FAO assay. The mitochondrial and peroxisomal FAO activities were determined by using labeled [1-^{14}C]palmitic acid (PA) (PerkinElmer) as a substrate, as reported in a previous study (21). For more details on FAO assay, see Supplemental Methods.

Glucose tolerance test

The glucose tolerance test (GTT) was performed according to the methods described previously (18, 32). Blood was collected from caudal vein and tails of Nile tilapia from Ctrl and MD treatments and from zebrafish from wt and *cpt1b*$^{-/-}$ mutants, respectively. For more details on the GTT see Supplemental Methods.

Nile tilapia primary hepatocytes culture and pharmacological inhibition

The isolation and culture of Nile tilapia primary hepatocytes were performed as previously described (21). After 12 h, all cells attached to the MD medium [Dulbecco modified Eagle medium (DMEM; Gibco); 10% fetal bovine serum (FBS; Gibco); 1 mM MD] and control medium (DMEM with 10% FBS). The cells were collected for FAO capacity assays after culture for 24 and 36 h. In this experiment, 3-well replicates were used for 1 treatment and the experiment was repeated 3 times. We further assayed several signaling proteins in Nile tilapia primary hepatocytes. The cells were preincubated with MD (1 mM) for 36 h and then treated individually with the following inhibitors for 24 h: 5 and 10 μM MK-2206 2HCl (MK; AKT pathway inhibitor; Selleckchem), or 1 μM rapamycin (Rap; mTOR inhibitor; LC Laboratories). The cells were then subjected to the cell viability measurement by using the MTT Assay Kits (Abcam) and related protein expressions by western blot analysis. For more details on cell culture process, see Supplemental Methods.

Insulin-stimulated glycogenesis test

Nile tilapia primary hepatocytes pretreated with MD medium for 36 h were prepared for an insulin-stimulated glycogenesis test. The ^{14}C-labeled glucose medium [5 mM D-glucose (Sangon Biotech) containing 2.5 μCi/mL D-[1-^{14}C]glucose (PerkinElmer)] was used to determine the glycogen labeling (33, 34). The MD-treated cells were incubated in the radioactive glucose medium for 4 h, with or without 100 nM insulin (Sigma). Cell lysates were prepared and cellular ^{14}C-labeled glycogen was collected after 75% ethanol precipitation and 1 N KOH dissolution as described previously (35). Finally, 200 μL [^{14}C]glycogen was transferred to a scintillation tube containing 2 mL scintillation cocktail medium (Ultima Gold XR; PerkinElmer) and assayed for radioactivity in a Tri-Carb 4910TR Liquid Scintillation Analyzer (PerkinElmer).

Metabolic tracking of FAs, glucose, and AAs

The Nile tilapia from Ctrl and MD treatments and zebrafish from wt and *cpt1b*$^{-/-}$ mutants were fasted for 12 h. Eighteen fish from each treatment were randomly sampled and used for metabolic tracking test. Six fish were randomly intraperitoneal (i.p.) injected with dimethyl sulphoxide (DMSO, Sigma, USA) containing [1-^{14}C]-PA (labeled 0.05 μCi/g body weight and unlabeled 1 μmol/kg body weight) (PerkinElmer, USA) (21, 28). Another 6 fish were injected with saline containing D-[1-^{14}C]-Glu (500 mg/kg body weight and 0.05 μCi/g body weight) (PerkinElmer, USA) (18), and the last six fish were injected with saline contain ^{14}C evenly labeled L-amino acid mixture (L-[^{14}C (U)]-AA, 500 mg/kg body weight and 0.05 μCi/g body weight) (PerkinElmer, USA) (22, 28). The total AA mixture was L-Lys, L-Arg, DL-Met, L-His and L-Val (2.7:2:1:1:1.3) (Sigma, USA) (22). The nutrient extraction was performed as described previously (34, 36). In addition, primary hepatocytes and dorsal muscle strips were isolated from Nile tilapia of Ctrl and MD treatments and prepared for glucose and AA oxidation measurements. The glucose and AA oxidation were measured by using D-[1-^{14}C]-Glu and L-[^{14}C (U)]-AA as described previously (6, 35). For more details on metabolic tracking test, see Supplementary Experimental Procedures.

Quantitative real-time PCR and mitochondrial cytochrome b DNA quantity measurement

The liver and muscle samples from 8 Nile tilapia of Ctrl and MD treatments, and from 18 zebrafish of wt and *cpt1b*$^{-/-}$ mutants, collected as described above, were used for total RNA isolation, cDNA synthesis, and quantitative real-time PCR (qRT-PCR) as described previously (37). The genes for β-actin 2 (*actb2*) and elongation factor 1a (*ef-1a*) of Nile tilapia, and for eukaryotic translation elongation factor 1α 1 (*eef1a1l1*) and actin α1b (*acta1b*) of zebrafish, were used as housekeeping gene controls for normalization of gene expressions. The details of primer sequences used in the present study are provided in **Supplemental Table 2** for Nile tilapia and in **Supplemental Table 3** for zebrafish. The qRT-PCR was conducted by using the $2^{-\Delta\Delta Ct}$ method:

$$\Delta Ct = Ct_{target} - (Ct_{EF1\alpha} + Ct_{\beta-actin})/2 \quad (1)$$

For more details of qRT-PCR see Supplemental Methods. We also evaluated the number of mitochondria by determining the quantity

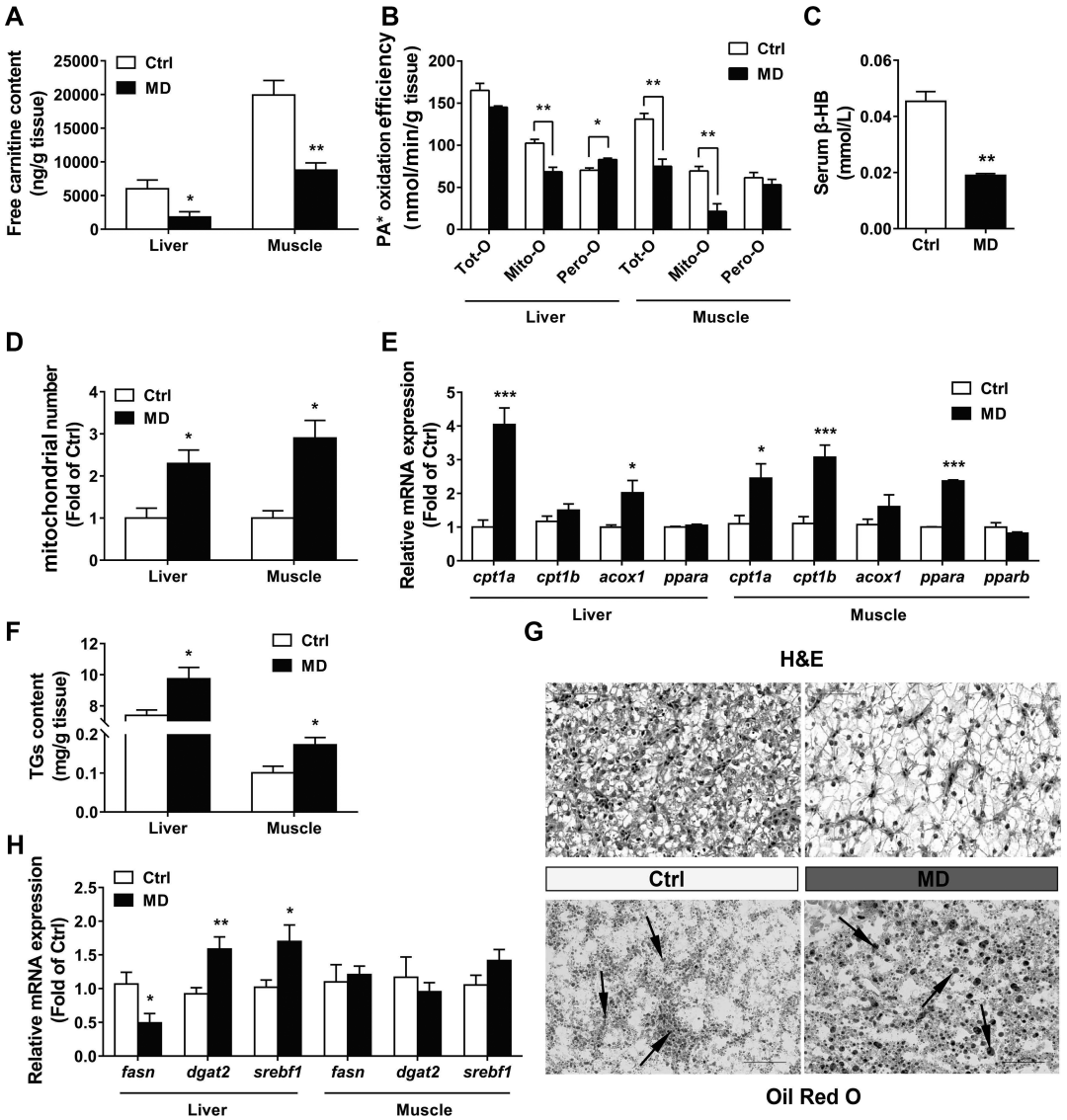

FIGURE 1 Free carnitine content (A), PA* β-oxidation efficiency (B), serum β-HB concentration (C), mitochondrial copy number (D), mRNA expression of FAO genes (E), TG content (F), H&E and Oil Red staining (G), and mRNA expression of lipogenetic genes (H) in liver and muscle of Nile tilapia fed Ctrl and MD diets for 6 wk. Values are mean ± SEM (free carnitine content and PA* β-oxidation efficiency: $n = 3$ replicates of 6 fish; serum β-HB concentration and TG content: $n = 6$ replicates of 6 fish; gene expression: $n = 8$ replicates of 8 fish). *,**,***Different from Ctrl: $^*P < 0.05$, $^{**}P < 0.01$, $^{***}P < 0.001$ (2-tailed independent *t* test). *acox1*, acyl-CoA oxidase 1; *cpt1a*, carnitine palmitoyltransferase 1a; *cpt1b*, carnitine palmitoyltransferase 1b; Ctrl, control group; *dgat2*, diglyceride acyltransferase 2; FAO, fatty acid β-oxidation; *fasn*, fatty acid synthase; H&E, hematoxylin-eosin; MD, mildronate group; Mito-O, mitochondrial oxidation; PA*, [1-^{14}C]palmitic acid; Pero-O, peroxisomal oxidation; *ppara*, peroxisome proliferator–activated receptor α; *pparb*, peroxisome proliferator–activated receptor β; *srebf1*, sterol regulatory element–binding transcription factor 1; TG, triglyceride; Tot-O, total oxidation; β-HB, β-hydroxybutyrate.

of mitochondrial cytochrome b (cytb) DNA. The total mitochondrial DNA was isolated from liver and muscle samples of 8 Nile tilapia in MD and Ctrl treatments, and 12 zebrafish of wt and *cpt1b*$^{-/-}$ mutants by using a TIANamp Marine Animals DNA Kit (Tiangen Biotech Co Ltd) by following the manufacturer's instructions. Relative copy number of mitochondrial DNA (mtDNA) was measured by qRT-PCR using mitochondrial cytb/β-action and cytb/β-globin for Nile tilapia (21) and zebrafish (22), respectively. Details of the primers are provided in **Supplemental Table 4** for Nile tilapia and **Supplemental Table 5** for zebrafish.

Transcriptomic analysis

Six liver samples of Nile tilapia from MD and Ctrl treatments were prepared for transcriptomic analysis. A paired-end RNA-seq sequencing library was sequenced by using the Illumina HiSeq 4000 (Illumina, Inc; 2 × 150 bp read length) after quantification by using TBS380 Fluorometer (Turner Biosystems Co. Ltd). The comparative analysis of differentially expressed genes (DEGs) and functional enrichment analysis of pathways were conducted as described previously (27). For more details on transcriptomic analysis, see Supplemental Methods.

Western blot analysis

Protein homogenates were prepared from 50 mg liver and muscle tissues in cell lysis buffer (Beyotime Biotechnology) containing 1 mM phenylmethanesulfonyl fluoride (Beyotime Biotechnology). Immunoblot analyses were performed by using standard procedures (21). The antibody information is provided in **Supplemental Table 6**. For more details on western blotting analysis, see Supplemental Methods.

Histological analyses

We examined the liver tissues of Nile tilapia from MD and Ctrl treatments by using Oil Red O staining method (38). Additionally,

hematoxylin and eosin staining of liver tissues was also performed by using paraffin-embedded tissues that were section-dried and stained using standard protocols (39). The digital images were examined under a Nikon Eclipse Ti-SR inverted microscope.

Statistical analyses

Results are presented as mean ± SEM. Data were tested for normality by using the Shapiro–Wilk test and for homogeneity of variance using the Levene test. A 2-tailed independent *t* test was performed to evaluate the significant differences (P values < 0.05) in measured parameters between the 2 groups. All analyses were conducted by using Statistical Package for the Social Science (SPSS) software version 19 for Windows (IBM SPSS).

Results

Carnitine-depleted Nile tilapia showed inhibited mitochondrial FAO

We first established the carnitine-depleted Nile tilapia model by feeding fish with the MD diet for 6 wk. The MD-treated fish had lower free carnitine contents in the liver and muscle by 81.9% and 56.0%, respectively, than Ctrl fish (**Figure 1**A). Accordingly, mitochondrial [1^{14}C]PA β-oxidation capacities were inhibited significantly in liver and muscle of MD-treated fish (Figure 1B) and in primary hepatocytes (**Supplemental Figure 1**A, B). The concentration of β-HB, a product of FAO in serum, was reduced in the MD-treated fish (Figure 1C). However, peroxisomal β-oxidation increased in the liver of the MD-treated fish (Figure 1B). The quantity of mitochondrial DNA of cytb, a marker for mitochondria numbers, increased significantly in the MD-treated fish (Figure 1D). Moreover, the MD-treated fish upregulated the expressions of the genes related to mitochondrial and peroxisomal FAO metabolism, such as *cpt1a*, *cpt1b*, and acyl-CoA oxidase 1 (*acox1*), in the liver and muscle (Figure 1E).

The MD-treated fish did not increase body weight compared with the Ctrl fish (**Table 1**), but accumulated more fat in the body and organs than Ctrl (Figure 1F, G; Table 1). Correspondingly, the mRNA expressions of TG synthesis genes such as diglyceride acyltransferase (*dgat2*) and sterol regulatory element–binding transcription factor 1 (*srebf1*) were upregulated, whereas fatty acid synthase (*fasn*) was downregulated in the liver of MD-treated fish (Figure 1H). The MD-treated and Ctrl fish had comparable serum AST and ALT activities (**Supplemental Figure 2**A), MDA concentration (Supplemental Figure 2B), and expressions of several inflammatory marker genes—heat shock protein 70 (*hsp70*), interleukin 10 (*il10*), interleukin 1β (*il1b*), and transforming growth factor β1 (*tgfb1*) (Supplemental Figure 2C). Together, these data indicate that the MD-treated fish had inhibited mitochondrial FAO, high body lipid accumulation, but no obvious tissue damage.

Inhibition of mitochondrial FAO improved insulin sensitivity and glucose utilization in Nile tilapia

The FAO-inhibited fish had lower serum glucose and insulin concentrations by 57.7% and 20.4%, respectively, than the Ctrl fish (Table 1). During the GTT, the FAO-inhibited fish showed faster glucose clearance (**Figure 2**A), and the serum insulin concentration in the FAO-inhibited fish was lower by 35–50% than Ctrl fish (Figure 2B), indicating improved insulin efficiency, but not insulin secretion. We further observed significantly higher insulin-stimulated glycogen synthetic efficiency in the Nile tilapia primary hepatocytes, which were pretreated with 1 mM MD for 36 h (Figure 2C). Furthermore, in the D-[1-^{14}C]glucose oxidation test, we found higher [^{14}C]carbon dioxide release from muscle strips of the MD-treated fish (Figure 2D) and MD-treated hepatocytes (**Supplemental Figure 3**A). In addition, the activities of key enzymes involved in glycolytic pathway such as HK and PK increased (**Supplemental Figure 4**A, B), whereas the glycogen concentrations in liver and muscle decreased in the FAO-inhibited fish (Figure 2E). Conversely, the hepatic contents of pyruvate (Figure 2F) and acetyl-CoA (Figure 2G) increased significantly in the FAO-inhibited fish, suggesting enhanced glycolysis and production of glycolysis-sourced acetyl-CoA.

In the FAO-inhibited fish, the mRNA expressions of insulin receptor a (*insra*) and glycolytic genes were upregulated; however, the expressions of gluconeogenic and glycogenic genes were downregulated compared with Ctrl (Figure 2H, I). Moreover, the phosphorylation of the α-subunit of AMPK (Thr172) and AKT (Ser473), and total AKT and insulin receptor (IR) proteins were all significantly higher in the liver of the FAO-inhibited fish than Ctrl (Figure 2J). Likewise, the phosphorylation of AKT (Ser473) and IR increased dramatically in the muscle of FAO-inhibited fish (Figure 2K). Similar results were also obtained in the Nile tilapia primary hepatocytes treated with 1 mM MD (Supplemental Figure 3B–D). Taken together, the FAO-inhibited fish showed enhanced glucose utilization, which resulted from improved insulin sensitivity rather than insulin secretion, and activation of AMPK/AKT pathways.

Inhibited mitochondrial FAO depressed AA catabolism and promoted protein deposition in Nile tilapia

We further found that the carcass ratio and the protein contents in the whole-fish body and muscle increased significantly in the FAO-inhibited fish (Table 1; **Figure 3**A). Serum TAA

TABLE 1 Effects of mildronate-induced carnitine depletion on growth performance, serum biochemical parameters, and body composition in Nile tilapia[1]

	Ctrl	MD
IBW, g/fish	4.28 ± 0.03	4.29 ± 0.03
FBW, g/fish	16.27 ± 0.74	17.06 ± 0.71
WG,[2] %	280 ± 18.7	298 ± 16.9
HSI,[3] %	2.34 ± 0.04	3.31 ± 0.18***
MFI,[4] %	0.33 ± 0.05	0.71 ± 0.12**
CR,[5] %	55.0 ± 1.32	61.3 ± 2.20*
Whole body composition		
TF, mg/g wet weight	44.8 ± 1.31	49.8 ± 0.82*
TP, mg/g wet weight	146 ± 0.85	152 ± 0.67**
Serum biochemical parameters		
NEFA, μmol/L	59.6 ± 1.03	134 ± 1.14***
TGs, mmol/L	0.45 ± 0.08	1.24 ± 0.24*
Glucose, mmol/L	5.48 ± 1.08	2.32 ± 0.26*
Insulin, nmol/L	33.9 ± 0.34	27.0 ± 1.17**
TAA, mmol/mL	0.17 ± 0.00	0.12 ± 0.00***

[1]Values are means ± SEM; $n = 3$ for IBW, FBW, and WG (3 replicates, 30 fish per replicate); $n = 8$ for HSI, MFI, and CR; $n = 5$ for TF and TP; $n = 6$ for serum biochemical parameters. *,**,***Significantly different from wildtype: $^*P \leq 0.05$, $^{**}P \leq 0.01$, and $^{***}P \leq 0.001$. CR, carcass ratio; Ctrl, control group; FBW, final mean body weight; HSI, hepatosomatic index; IBW, initial mean body weight; MD, mildronate group; MFI, mesenteric fat index; NEFA, nonessential fatty acid; TAA, total amino acids; TF, total fat; TGs, triglycerides; TP, total protein; WG, weight gain.
[2]WG = 100 × (FBW − IBW)/IBW.
[3]HSI = 100 × (liver weight/body weight).
[4]MFI = 100 × (mesenteric fat weight/body weight).
[5]CR = 100 × (carcass weight/body weight).

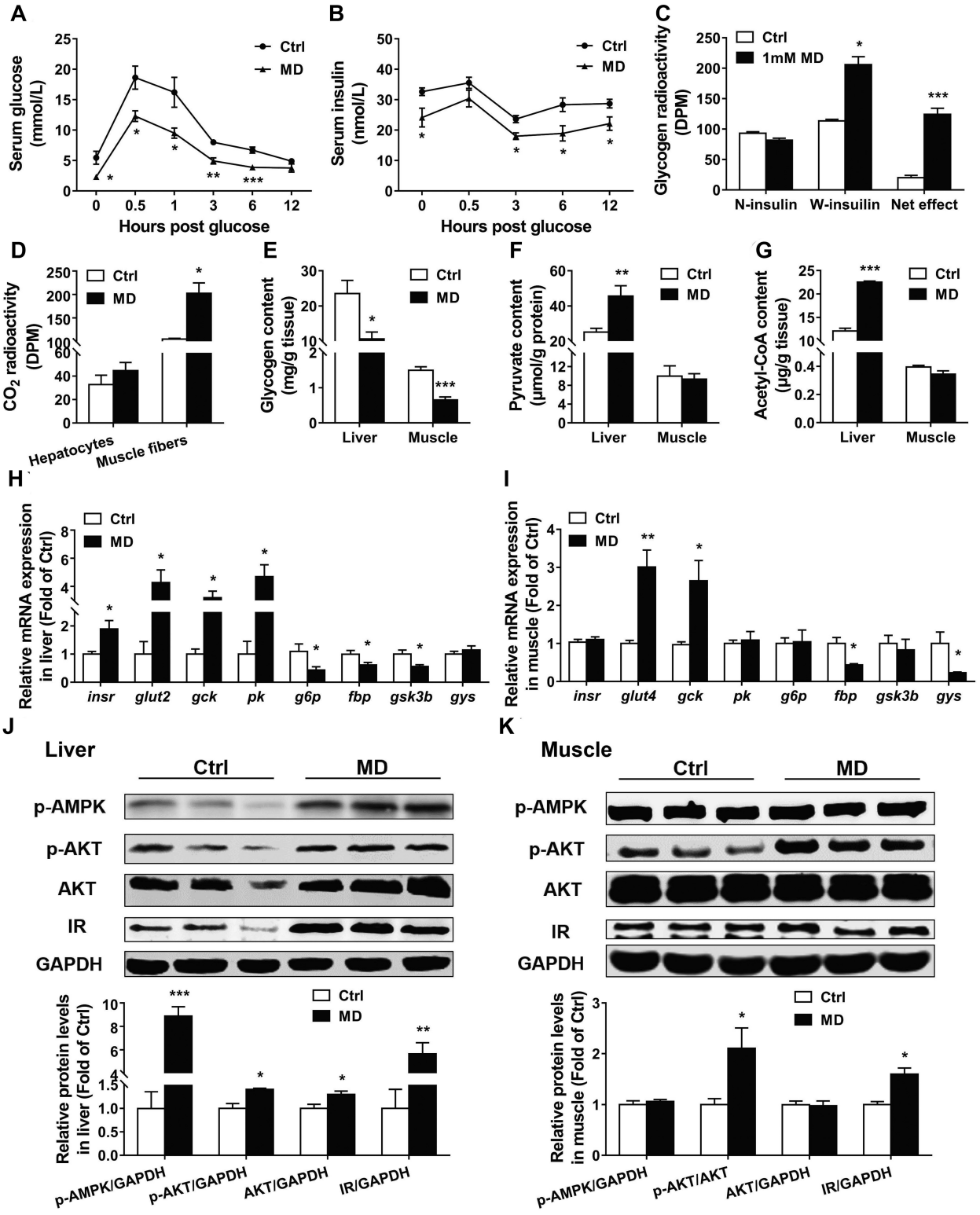

FIGURE 2 Serum glucose (A) and insulin (B) concentration in GTT, glycogen radioactivity of primary hepatocytes from Nile tilapia with 1 mM MD treatment for 36 h (C), carbon dioxide radioactivity released from D-[1-^{14}C]glucose oxidation of Nile tilapia primary hepatocytes and muscle strips (D), glycogen (E), pyruvate (F), and acetyl-CoA (G) content, gene expression of genes related to carbohydrate metabolism (H–I), and protein expression of insulin pathway (J–K) in liver and muscle of Nile tilapia fed Ctrl and MD diets for 6 wk. Values are mean ± SEM (GTT: $n = 5$ replicates of 5 fish; glycogen radioactivity: $n = 3$; carbon dioxide radioactivity: $n = 6$; glycogen and pyruvate content: $n = 6$ replicates of 6 fish; acetyl-CoA content and protein expression: $n = 3$ replicates of 6 fish; gene expression: $n = 8$ replicates of 8 fish). *,**,***Different from Ctrl: $^{*}P < 0.05$, $^{**}P < 0.01$, $^{***}P < 0.001$ (2-tailed independent *t* test). AKT, protein kinase B; Ctrl, control group; DPM, disintegrations per minute; *fbp*, fructose-1,6-bisphosphatase; *g6p*, glucose-6-phosphatase; GAPDH, glyceraldehyde-3-phosphate dehydrogenase; *gck*, glucokinase; *glut*, glucose transporter; *gsk3b*, glycogen synthase kinase 3β; GTT, glucose tolerance test; *gys*, glycogen synthase; *insr* and IR, insulin receptor; MD, mildronate group; N-insulin, no insulin; p-AKT, phosphorylation of protein kinase B; p-AMPK, phosphorylation of adenosine 5′-monophosphate–activated protein kinase; *pk*, pyruvate kinase; W-insulin, with insulin.

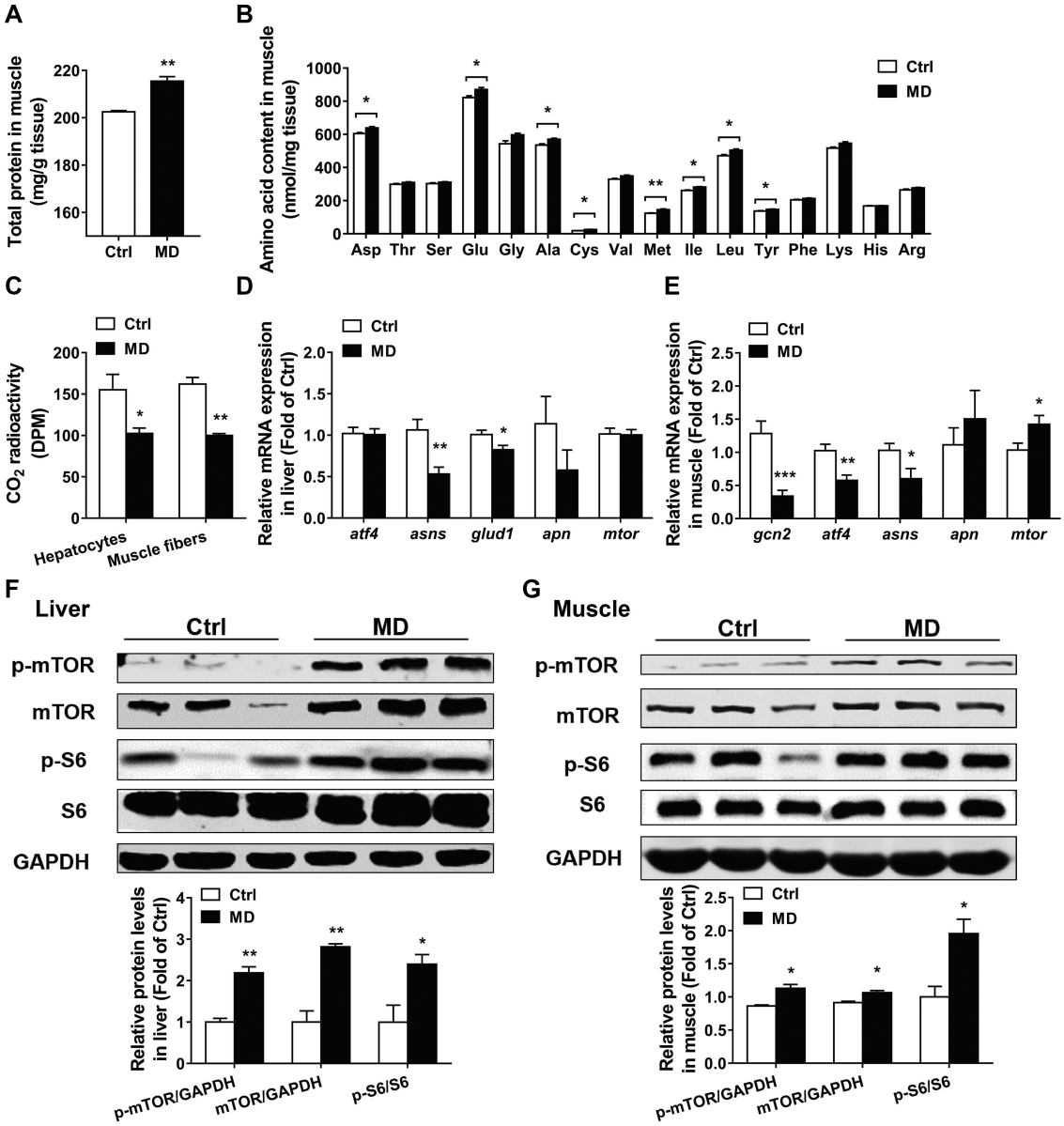

FIGURE 3 Total protein (A) and amino acid content (B) in muscle, carbon dioxide radioactivity released from L-[^{14}C (U)]-amino acid oxidation of Nile tilapia primary hepatocytes and muscle strips (C), mRNA expression of genes involved in protein metabolism (D, E), and protein expression of mTOR pathway (F, G) in liver and muscle of Nile tilapia fed Ctrl and MD diets for 6 wk. Values are mean ± SEM (total protein, amino acid content, and protein expression: $n = 3$ replicates of 6 fish; carbon dioxide radioactivity: $n = 6$; gene expression: $n = 8$ replicates of 8 fish). *,**,***Different from Ctrl: *$P < 0.05$, **$P < 0.01$, ***$P < 0.001$ (2-tailed independent *t* test). *apn*, aminopeptidase N; *asns*, asparagine synthetase; *atf4*, activating transcription factor 4; Ctrl, control group; DPM, disintegration per minute; GAPDH, glyceraldehyde-3-phosphate dehydrogenase; *gcn2*, general control nonderepressible 2; *glud1*, glutamate dehydrogenase 1; MD, mildronate group; mTOR, mechanistic target of rapamycin kinase; p-mTOR, phosphorylation of mechanistic target of rapamycin kinase; p-S6, phosphorylation of S6 ribosomal protein; S6, S6 ribosomal protein; L-[^{14}C (U)]-amino acids, 14C evenly labeled L-amino acids mixture.

concentration was reduced in the FAO-inhibited fish (Table 1), suggesting more AAs were deposited in the body. As direct evidence, most AAs were elevated significantly in the muscle of the FAO-inhibited fish compared with Ctrl (Figure 3B). We next measured the oxidation of L-[^{14}C (U)]-AA in primary hepatocytes and muscle strips isolated from the FAO-inhibited fish and Ctrl. Results indicated that the production of [^{14}C]carbon dioxide decreased significantly in the FAO-inhibited fish compared with Ctrl fish (Figure 3C; Supplemental Figure 3A). The mRNA expressions of a peptide hydrolysis gene, aminopeptidase N (*apn*), and AA catabolism genes such as asparagine synthetase (*asns*) and glutamate dehydrogenase 1 (*glud1*), were reduced in the liver (Figure 3D), and other AA catabolic genes, including general control nonderepressible 2 (*gcn2*), activating transcription factor 4 (*atf4*), and *asns* were downregulated in the muscle in the FAO-inhibited fish (Figure 3E).

Furthermore, we found that the protein levels of total mTOR, phosphorylation of mTOR (Ser2448), and S6 ribosomal protein (S6) (Ser235/236) were dramatically higher in the liver (Figure 3F) and muscle (Figure 3G) of the FAO-inhibited fish than Ctrl. Similarly, we also found elevated phosphorylation of S6 (Ser235/236) in the primary hepatocytes pretreated with 1 mM MD (Supplemental Figure 3C, D), suggesting activation

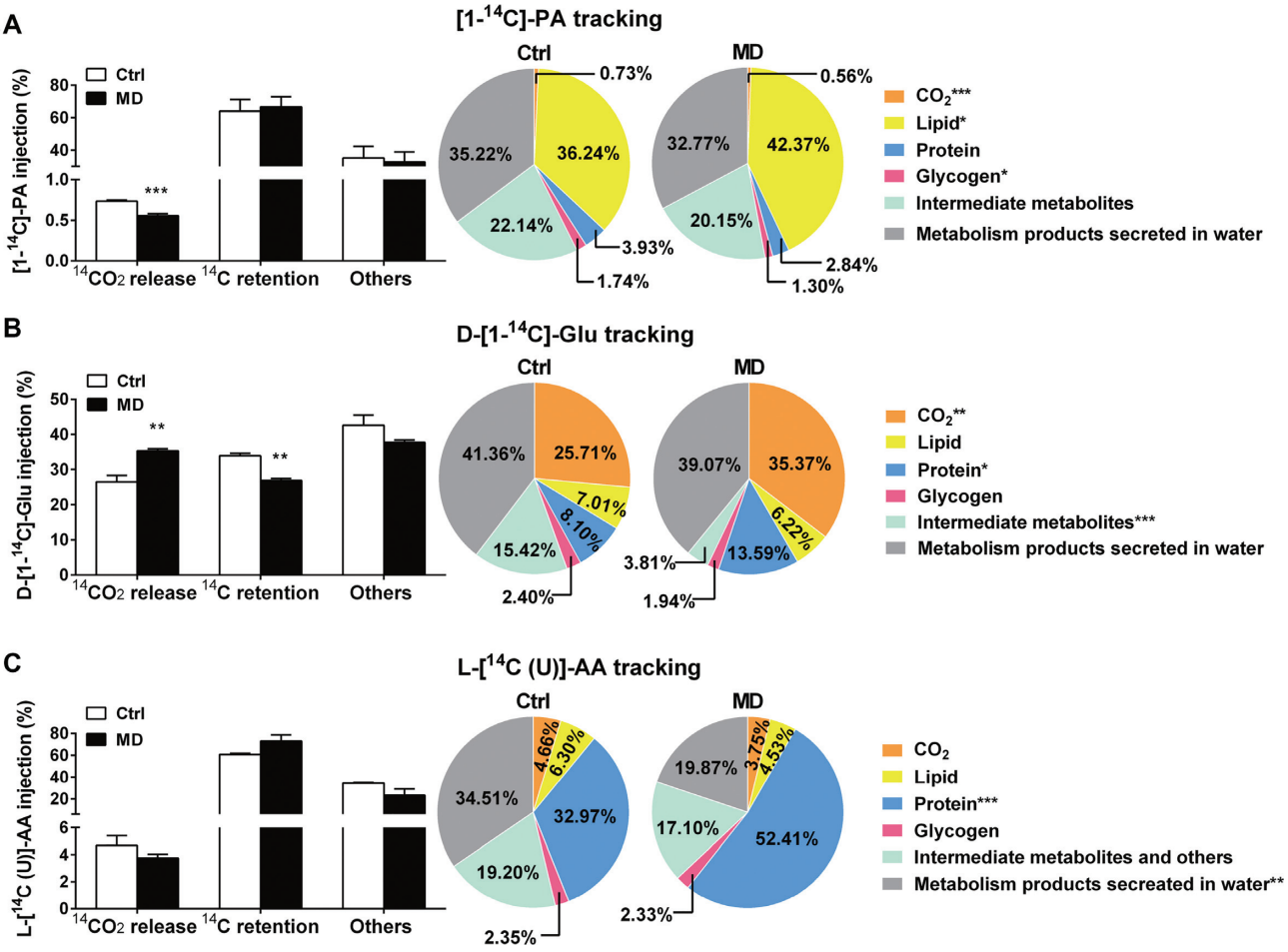

FIGURE 4 Metabolic tracking of [1 ^{14}C]-PA (A), D-[1-^{14}C]glucose (B), and L-[^{14}C (U)]-AA (C) in Nile tilapia fed Ctrl and MD diets for 6 wk. Values are mean ± SEM, $n = 6$. *,**,***Different from Ctrl: *$P < 0.05$, **$P < 0.01$, ***$P < 0.001$ (2-tailed independent t test). AA, amino acid; Ctrl, control group; Glu, glucose; L-[^{14}C (U)]-AA, 14C evenly labeled L-amino acids mixture; MD, mildronate group; PA, palmitic acid.

of the mTOR pathway. These findings indicate that mitochondrial FAO inhibition remodeled energy metabolism, which induced protein deposition from depressed AA breakdown and improved protein synthesis due to activation of the mTOR pathway.

Inhibited mitochondrial FAO remodeled nutrient metabolism in Nile tilapia

To understand precisely the mechanisms by which mitochondrial FAO inhibition remodeled nutrient homeostasis, we intraperitoneally injected fish individually using ^{14}C-labeled PA, glucose, and AA mixture. After injection of [1-^{14}C]-PA, we found less release of [^{14}C]carbon dioxide, significantly increased ^{14}C-lipid, and decreased [^{14}C]glycogen in the FAO-inhibited fish (**Figure 4**A). This indicates that the FAO-inhibited fish esterified more of the ingested FA to lipid, but oxidized less FA to form carbon dioxide, and that the conversion of FA into other nutrients, such as glycogen, was also lowered. After [1-^{14}C]glucose injection, a large portion (25.71–35.37%) of ^{14}C was recovered in the released [^{14}C]carbon dioxide in both fish groups, whereas the FAO-inhibited fish released higher [^{14}C]carbon dioxide and retained less ^{14}C in the body than the Ctrl fish (Figure 4B). More precisely, we found a 68% significantly higher ^{14}C-protein deposition ratio in the FAO-inhibited fish (13.59% compared with 8.10%), but lower proportion of [^{14}C]glycogen was observed in the FAO-inhibited fish (1.94% compared with 2.40%) than in Ctrl fish (Figure 4B). This indicates that more ingested glucose was oxidized to supply energy in the FAO-inhibited fish, and concurrently more glucose was used to synthesize protein in these fish.

The intraperitoneal L-[^{14}C (U)]-AA injection test indicated that the release of [^{14}C]carbon dioxide in the FAO-inhibited fish was lower (3.75% compared with 4.66%), and a significantly larger proportion of ^{14}C-protein was found in the FAO-inhibited fish than in the Ctrl (52.41% compared with 32.97%) (Figure 4C). This clearly indicates that the mitochondrial FAO-inhibited fish preferentially used the ingested AA for protein synthesis, rather than oxidizing them for energy generation. In general, these results provide compelling evidence that mitochondrial FAO inhibition in fish remodels nutrient metabolism by elevating utilization of glucose as the major metabolic fuel, preserving AAs from degradation and promoting protein synthesis from AAs and other metabolic intermediates.

Inhibited mitochondrial FAO changed energy homeostasis through activation of AKT-mTOR pathways

We conducted transcriptomic analyses to obtain a systemic overview of energy metabolism in the FAO-inhibited Nile tilapia liver. There were 411 DEGs between the FAO-inhibited fish and Ctrl (**Supplemental Figure 5**A), and most of the enriched DEGs

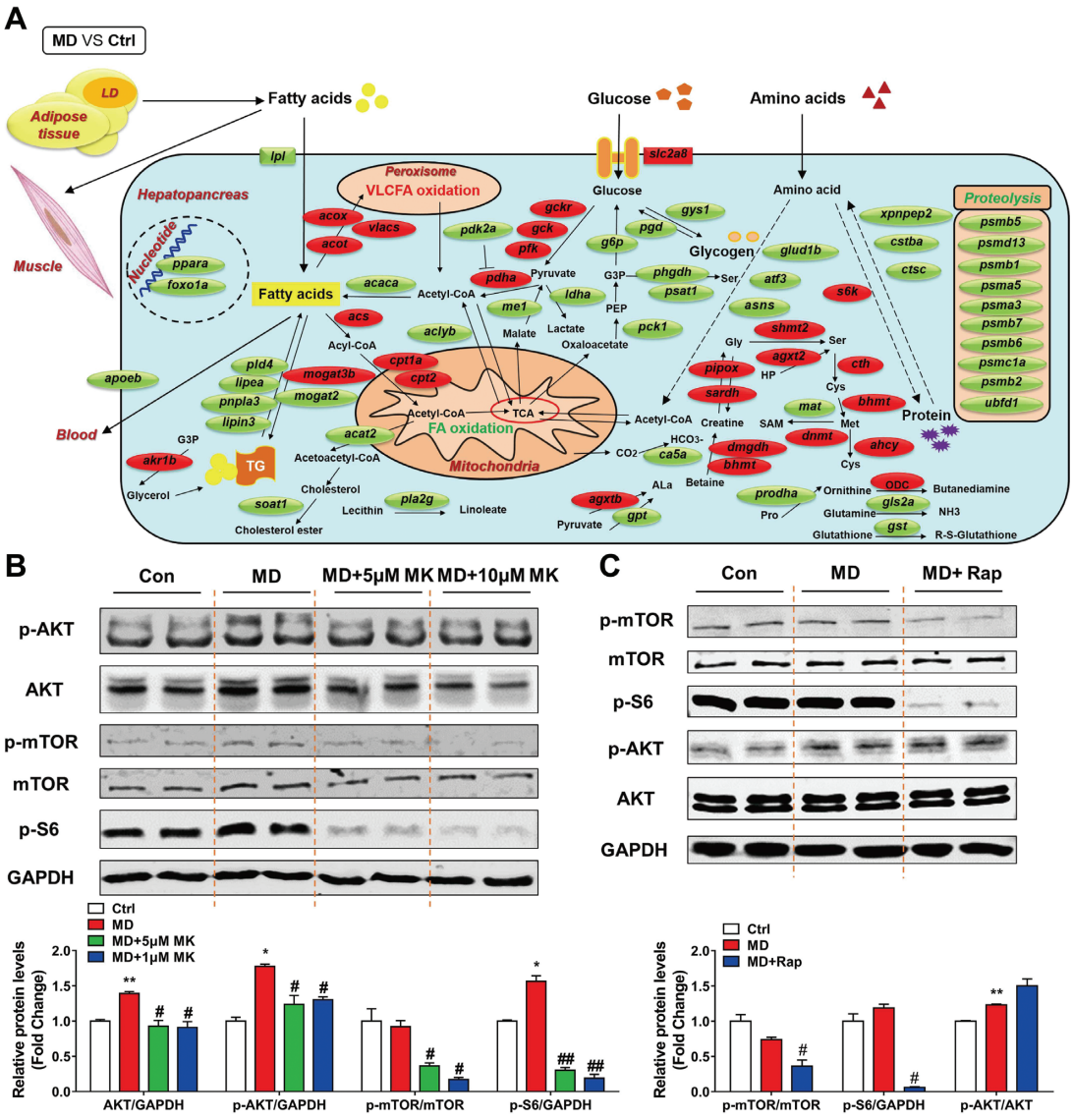

FIGURE 5 Differentially expressed genes involved in metabolic pathways in hepatic transcriptomic analysis of Nile tilapia fed Ctrl and MD diets for 6 wk (A), and protein expression analysis of AKT (B) and mTOR (C) pathways in Nile tilapia primary hepatocytes. (A) Red and green colors indicate upregulated and downregulated genes, respectively; abbreviations are defined in **Supplemental Figure Caption**. (B) Nile tilapia primary hepatocytes treated with 1 mM MD, 1 mM MD + 5 μM MK, and MD + 10 μM MK for 24 h. (C) Nile tilapia primary hepatocytes treated with 1 mM MD, 1 mM MD + 1 μM Rap for 24 h. Values are mean ± SEM (transcriptomic analysis: $n = 3$ of replicates of 6 fish; protein expression: $n = 3$ of cell wells from the six-well plates per condition). *,**Different from Ctrl: $^{*}P < 0.05$ and $^{**}P < 0.01$ (2-tailed independent *t*-test). $^{\#,\#}$Different from MD: $^{\#}P < 0.05$ and $^{\#}P < 0.01$ (2-tailed independent *t* test). AKT, protein kinase B; Ctrl or Con, control group; GAPDH, glyceraldehyde-3-phosphate dehydrogenase; MD, mildronate group; MK, MK-2206 2HCl; mTOR, mechanistic target of rapamycin kinase; p-AKT, phosphorylation of protein kinase B; p-mTOR, phosphorylation of mechanistic target of rapamycin kinase; p-S6, phosphorylation of S6 ribosomal protein; Rap, rapamycin.

were involved in energy metabolism (Supplemental Figure 5B). We next classified the DEGs associated with lipid, glucose, and protein metabolism (Supplemental Figure 5C) and generated a schematic illustration of DEGs in significantly changed metabolic pathways (Figure 5A). Briefly, the FAO-inhibited fish downregulated the genes involved in lipid hydrolysis and FA synthesis, and upregulated the genes involved in lipogenesis and mitochondrial and peroxisomal FAO. The FAO-inhibited fish also increased expression of the genes associated with glycolysis and pyruvate dehydrogenase E1 component subunit α (*pdha*), which catalyzes pyruvate breakdown to acetyl-CoA, and conversely downregulated genes related to gluconeogenesis, glycogen synthesis, lactate production, and pyruvate dehydrogenase kinase 2A (*pdk2a*). Notably, prominent differences were detected in the genes related to protein metabolism, including decreased proteolysis in ubiquitin-proteasome, peptide hydrolysis, and AA breakdown, and increased expressions of genes related to AA conversion.

The results from previous sections in the present study confirmed that inhibited mitochondrial FAO caused a compensatory increase in glucose utilization and protein deposition, and the AKT and mTOR signaling pathways were both stimulated. To understand the relation between AKT and mTOR signaling pathways in remodeling energy metabolism, we further measured the activities of AKT and mTOR in the presence of specific antagonists, MK and Rap, respectively, in

TABLE 2 The growth performance and serum biochemical parameters in wt and *cpt1b*$^{-/-}$ zebrafish[1]

	Wt	*cpt1b*$^{-/-}$
IBW, mg/fish	162 ± 2.87	154 ± 3.52
FBW, mg/fish	269 ± 2.40	269 ± 6.50
WG,[2] %	69.9 ± 0.45	77.0 ± 0.10***
FBL, cm/fish	2.88 ± 0.08	2.91 ± 0.05
CF,[3] %	0.77 ± 0.02	0.92 ± 0.03***
VSI,[4] %	9.49 ± 0.44	11.0 ± 0.26*
CR,[5] %	57.3 ± 0.78	61.5 ± 1.09**
Serum glucose, mmol/L	4.58 ± 0.14	3.68 ± 0.13**
Serum insulin, nmol/L	185 ± 6.02	142 ± 6.66**

[1]Values are means ± SEM; $n = 3$ for IBW, FBW, and WG (3 replicates, 38 fish per replicate); $n = 12$ for FBL, CF, and CR; $n = 6$ for VSI; $n = 4$ for serum glucose and insulin concentration. *,**,***Significantly different from wildtype: *$P \leq 0.05$, **$P \leq 0.01$, and ***$P \leq 0.001$. CF, condition factor; *cpt1b*, carnitine-palmitoyl transferase 1b; CR, carcass ratio; FBL, final body length; FBW, final mean body weight; IBW, initial mean body weight; VSI, viscerosomatic index; WG, weight gain; wt, wildtype.
[2]WG = 100 × (FBW − IBW)/IBW.
[3]CF = 100 × (body weight, g)/(body length, cm)^3.
[4]VSI = 100 × (viscera weight/body weight).
[5]CR = 100 × (carcass weight/body weight).

primary Nile tilapia hepatocytes pretreated with 1 mM MD or not. After the MD treatment, the AKT, phosphorylation of protein kinase B (p-AKT), and phosphorylation of S6 ribosomal protein (p-S6) protein levels were elevated significantly in cells (Figure 5B). However, the MK treatment suppressed significantly the protein levels of AKT, p-AKT, p-mTOR, and p-S6 in the MD-treated cells (Figure 5B), suggesting that the inhibited FAO-induced mTOR activity is dependent on AKT activity. In contrast, the Rap-induced inhibition of mTOR did not suppress the MD-elevated expression of p-AKT (Figure 5C), suggesting that AKT activation is independent of the mTOR pathway in the MD-treated cells. These findings suggest that the mitochondrial FAO inhibition reconstructed the systemic nutrient metabolism to maintain energy homeostasis. Moreover, increased protein synthesis was a consequence of the stimulated glucose utilization through AKT-mTOR pathways.

cpt1b deletion remodeled energy metabolism and promoted protein deposition in zebrafish

The *cpt1b* gene is one of the key enzymes involved in mitochondrial FAO and is highly expressed in muscle and liver of zebrafish (**Supplemental Figure 6**A). To further confirm the effects of mitochondrial FAO inhibition on energy homeostasis and protein deposition, as an alternative to the pharmacological treatment, we knocked out the *cpt1b* gene in zebrafish by using CRISPR/Cas9 (Supplemental Figure 6B–D). The *cpt1b*$^{-/-}$ zebrafish larvae had lower swimming activity and OCR, and higher MFI (Supplemental Figure 6E–G), suggesting that *cpt1b*$^{-/-}$ fish had a lower metabolic rate and movement compared with wt fish. Next, we fed the adult *cpt1b*$^{-/-}$ and wt zebrafish a normal diet containing 8% fat. After feeding for 4 wk, the *cpt1b*$^{-/-}$ zebrafish gained more body weight than wt fish but had similar body length as the wt fish (**Table 2**). The *cpt1b*$^{-/-}$ zebrafish also had lower mitochondrial FAO, higher peroxisome FAO (**Figure 6**A), and greater fat accumulation in liver, muscle, and visceral mass (Figure 6B; **Supplemental Figure 7**A), and increased hepatic mitochondrial copy number compared with wt fish (Supplemental Figure 7B). The mRNA expressions of the genes related to FAO and lipogenesis were upregulated in the liver of the *cpt1b*$^{-/-}$ zebrafish compared with wt fish (Supplemental Figure 7C, D). These results demonstrate that the *cpt1b*$^{-/-}$ zebrafish had similar changes in lipid metabolism as the carnitine-depleted Nile tilapia.

We further observed that the *cpt1b*$^{-/-}$ zebrafish had lower serum glucose and insulin concentrations (Table 2), but had higher acetyl-CoA and pyruvate contents in the muscle than wt fish (**Supplemental Figure 8**A, B). The lactate contents were similar between *cpt1b*$^{-/-}$ zebrafish and wt fish, both in the liver and muscle (Supplemental Figure 8C). The *cpt1b*$^{-/-}$ zebrafish also showed improved glucose clearance during the GTT (Figure 6C), and had lower hepatic and muscle glycogen contents than wt fish (Figure 6D). Subsequently, the expressions of glycolysis and glucose transport genes were upregulated in the *cpt1b*$^{-/-}$ zebrafish, yet genes related to gluconeogenesis and glycogen synthesis were downregulated (Supplemental Figure 8D, E). Moreover, the levels of AKT phosphorylation at Ser473 were significantly higher in both liver and muscle in the *cpt1b*$^{-/-}$ zebrafish than wt fish (Figure 6E). These findings suggest that the *cpt1b*$^{-/-}$ fish increased glucose utilization through activation of the insulin signaling pathway.

The *cpt1b*$^{-/-}$ zebrafish also had elevated carcass ratio (Table 2), body protein (Figure 6F), and muscle AA contents, especially the branched-chain AA, including valine and leucine (**Supplemental Figure 9**). Correspondingly, the *cpt1b*$^{-/-}$ zebrafish had lower expressions of the genes related to AA catabolism than wt fish (Figure 6G). The phosphorylation of mTOR was also activated in the *cpt1b*$^{-/-}$ zebrafish (Figure 6H). These results illustrate that the *cpt1b*$^{-/-}$ zebrafish had lower AA catabolism and higher protein synthesis ability than the wt zebrafish.

We next performed the ^{14}C-labeled nutrient tracking test in the *cpt1b*$^{-/-}$ zebrafish and wt fish (**Supplemental Figure 10**A–C). In the *cpt1b*$^{-/-}$ fish, more [1-^{14}C]-PA was esterified and converted for protein synthesis, but less was oxidized; more D-[1-^{14}C]glucose was oxidized as a fuel, and used for synthesis of protein, but not glycogen; and less L-[^{14}C (U)]-AA was oxidized compared with wt fish. Altogether, these data indicate that the inhibition of mitochondrial FAO, by either biochemical activity or gene knockout, triggers a compensatory increase in glycolysis but reduces protein catabolism and elevates protein synthesis, causing higher protein deposition.

Discussion

In the present study, we generated 2 mitochondrial FAO–inhibited fish models: carnitine-depleted Nile tilapia and *cpt1b*-deficient zebrafish. These fish models showed similar moderate lipid accumulation, with induced compensatory metabolic responses, including increased peroxisomal fatty acid oxidation, mitochondrial biogenesis, and FAO gene expressions. These results accord with those obtained in mammalian models with mitochondrial FAO deficiency (6–8), verifying the similar phenotypes in lipid metabolism in mitochondrial FAO–inhibited animals. However, to the best of our knowledge, our present study indicates for the first time that energy homeostasis regulation is a promising strategy for protein production in cultured animals, at least in fish. The mechanisms summarizing the systemic remodeling of energy homeostasis caused by the inhibition of mitochondrial FAO are illustrated in **Figure 7**.

In response to a dynamic nutrient environment, cells need to precisely sense their physiological states and remodel metabolic

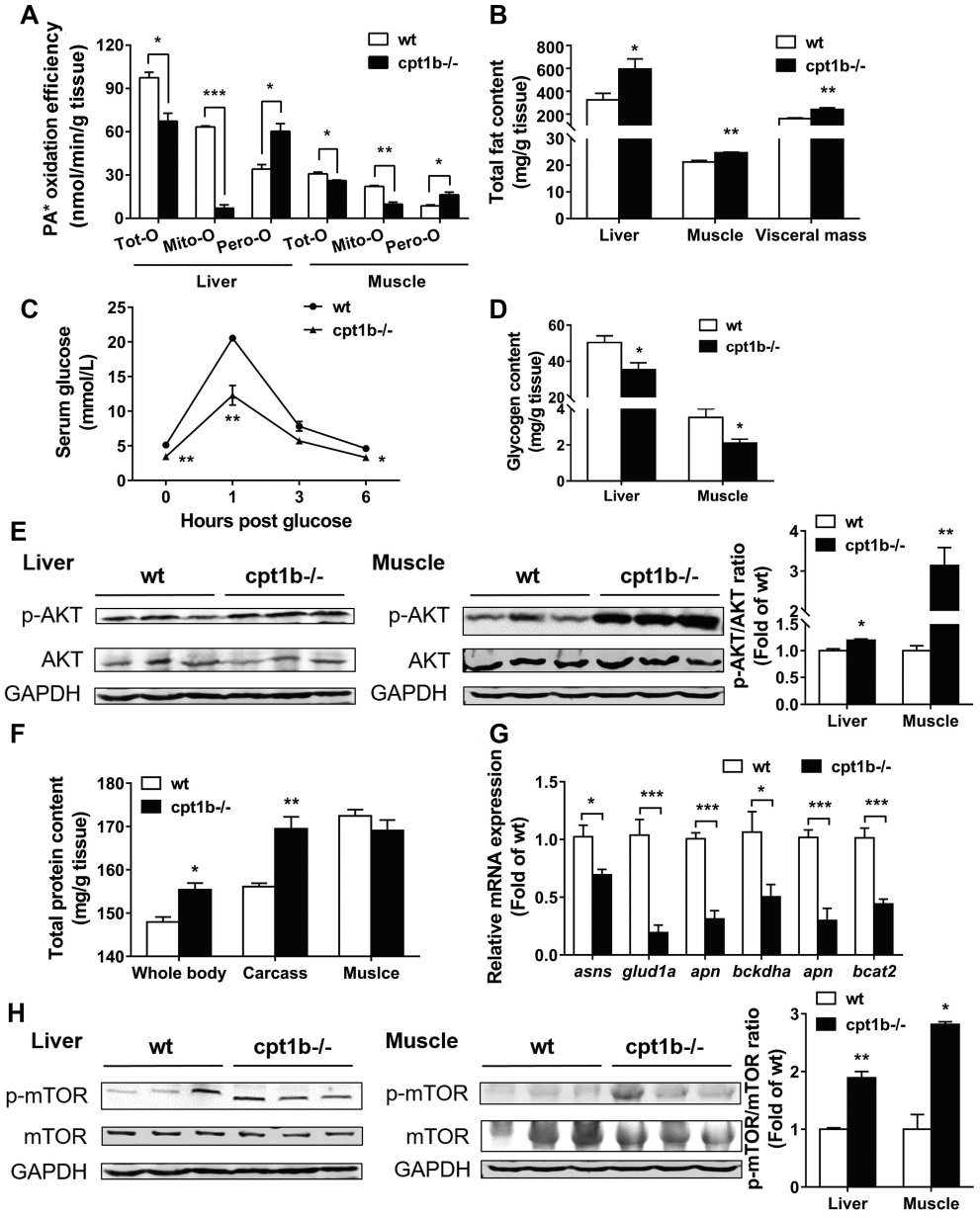

FIGURE 6 The PA* β-oxidation efficiency (A), total fat content (B), serum glucose concentration in GTT (C), glycogen content (D), protein expression of p-AKT and AKT (E), total protein content (F), mRNA expression of genes related to amino acid catabolism (G), and protein expression of p-mTOR and mTOR (H) in tissues of wt and *cpt1b*$^{-/-}$ zebrafish. Values are mean ± SEM (PA* β-oxidation efficiency and protein expression: $n = 3$ replicates of 9 fish; total fat content: $n = 3$ replicates of 18 fish; GTT: $n = 5$ replicates of 15 fish; glycogen content and gene expression: $n = 6$ replicates of 18 fish). *,**,***Different from wt, $^{*}P < 0.05$, $^{**}P < 0.01$, $^{***}P < 0.001$ (2-tailed independent *t* test). AKT, protein kinase B; *apn*, aminopeptidase N; *asns*, asparagine synthetase; *bcat2*, branched-chain amino-acid transaminase 2; *bckdha*, branched-chain keto-acid dehydrogenase E1 subunit α; *cpt1b*$^{-/-}$, *cpt1b* knockout zebrafish; GAPDH, glyceraldehyde-3-phosphate dehydrogenase; *glud1a*, glutamate dehydrogenase 1a; GTT, glucose tolerance test; Mito-O, mitochondrial oxidation; mTOR, mechanistic target of rapamycin kinase; PA*, [1-^{14}C]palmitic acid; p-AKT, phosphorylation of protein kinase B; Pero-O, peroxisomal oxidation; p-mTOR, phosphorylation of mechanistic target of rapamycin kinase; Tot-O, total oxidation; wt, wild-type zebrafish.

patterns in order to maintain energy homeostasis. Lipid and carbohydrate metabolism is the main source of mitochondrial acetyl-CoA production required for energy homeostasis (40, 41). Accumulating evidence indicates that the rate of acetyl-CoA production originating from FA and glucose oxidation relies closely on the size of the mitochondrial acetyl-CoA pool, which fluctuates depending on intracellular metabolic states (41, 42). AMPK is an intracellular energy sensor required to regulate energy metabolism (43, 44), and is activated when cells are in a poor nutritional state by switching on catabolic pathways, such as FAO and glycolysis, while switching off energy-consuming processes such as FA and cholesterol biosynthesis (45, 46). In the present study, mitochondrial FAO inhibition reduced the concentrations of acetyl-CoA from lipid catabolism, mimicking a low-energy state that activated AMPK to shift energy metabolism from lipid catabolism to glucose oxidation to maintain cellular energy homeostasis. In contrast, our previous studies showed that enhanced lipid catabolism, either through activation of peroxisome proliferator–activated receptor α or exogenous L-carnitine supplementation, reduced

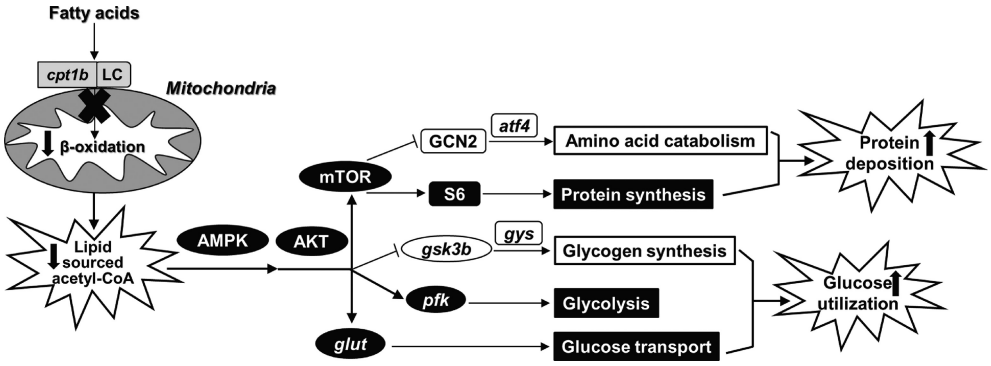

FIGURE 7 The systemic remodeling of energy homeostasis caused by the inhibition of mitochondrial FAO. Mitochondrial FAO inhibition through low-carnitine conditions or *cpt1b* deficiency significantly reduced lipid-sourced acetyl-CoA, which activated the AMPK/AKT-mTOR pathways. To maintain cellular energy homeostasis, glucose uptake and glycolysis were increased, whereas glycogen synthesis was reduced, resulting in an elevated flux of glucose-sourced acetyl-CoA. Meanwhile, AA-sourced acetyl-CoA was decreased due to the increase in protein synthesis and the decrease in AA catabolism, contributing to high protein deposition. AA, amino acid; AKT, protein kinase B; AMPK, adenosine 5′-monophosphate–activated protein kinase; *atf4*, activating transcription factor 4; *cpt1b*, carnitine-palmitoyl transferase 1b; GCN2, general control nonderepressible 2; glut, glucose transporter; *gsk3b*, glycogen synthase kinase 3*β*; *gys*, glycogen synthase; LC, L-carnitine; mTOR, mechanistic target of rapamycin kinase; *pfk*, phosphofructokinase; S6, ribosomal protein S6.

the expressions of glycolytic genes and increased glycogen deposition in fish (20, 21). These studies confirm that FA and glucose oxidation synergistically maintain stable energy supply in fish. Similarly, studies have consistently found beneficial effects of mitochondrial FAO inhibition by naturally shifting the substrate selection that favors glucose utilization in mammals (6–9, 47). Other mammalian studies also revealed that the reduction of glucose oxidation, through inhibition of sodium-dependent glucose transporter 2 (10) or overexpression of pyruvate dehydrogenase kinase 4 (11), increased lipid oxidation for energy supply. Of note, compared with mammals, fish are traditionally considered inefficient in utilizing glucose for a fuel and prefer to use protein as the main energy source (16, 17). However, the present study indicates that mitochondrial FAO–inhibited fish potentially enhance carbohydrate utilization to maintain energy homeostasis, when energy supply from other nutrients, such as lipids, is inhibited. From an evolutionary adaptation perspective, our results suggest that the ability of fish to utilize glucose and carbohydrate is depressed by lipid metabolism in normal situations, because in natural aquatic environments the foods of most fish contain more lipid than carbohydrate, especially for carnivorous or omnivorous fish.

In fish, some studies have demonstrated that the pharmacological activation of AMPK stimulates glucose uptake and utilization (48–50), through modulation of insulin sensitivity (51, 52). In the present study, we found that the mitochondrial FAO inhibition decreased blood glucose and insulin concentrations and glycogen content in tissues. In addition, an increase in glucose clearance in vivo was detected in the mitochondrial FAO–inhibited fish by using the GTT, and insulin sensitivity was enhanced in vitro by using the insulin-stimulated glycogen synthetic efficiency test. Moreover, during the ^{14}C-labeled glucose tracking test, the mitochondrial FAO–inhibited fish elevated their glucose oxidation capacity. These data strongly suggest that glucose oxidation and insulin sensitivity were improved in the mitochondrial FAO–inhibited fish, in line with the data obtained from mice (6, 8, 53). Accumulating evidence indicates that high insulin sensitivity promotes glycolysis (54) and upregulates the expressions of insulin receptors and glucose transporters, which are tightly correlated with increased cellular glucose uptake (55, 56). Correspondingly, the expressions of the genes associated with glucose uptake and glycolysis were upregulated in the mitochondrial FAO–inhibited fish. Moreover, the activity of AKT protein, which has been implicated in the insulin signaling pathway (46, 57), was enhanced to increase the insulin sensitivity, which elevated glucose uptake and glycolysis and decreased glycogen synthesis. Therefore, mitochondrial FAO inhibition initially induces an energy-exhausted state, which triggers glucose utilization via the activation of AMPK/AKT pathways.

Our findings from the present study showed that mitochondrial FAO inhibition also promoted protein deposition. A series of mammalian and fish studies have reported that the AKT-mTOR pathways induce a phosphorylation cascade, which results in accelerating protein synthesis and inhibition of proteolysis in muscle (13, 58). The present work further indicated that, accompanied by the activation of AKT protein, the mTOR pathway was also activated in the tissues in the mitochondrial FAO–inhibited fish, leading to an increase in whole-body protein content and a decrease in the ^{14}C-labeled AA oxidation. In addition, the mTOR pathway can also be activated in the presence of nutrients (nutrition-rich status), which promotes conversion of excess intermediate metabolites into AAs required to participate in protein synthesis (59). During our D-[1-^{14}C]glucose tracking test, more ^{14}C-protein was deposited in the mitochondrial FAO–inhibited fish, suggesting an accelerated glucose breakdown, the substrates of which promote protein synthesis. Moreover, the transcriptomic results also revealed that the expressions of protein catabolism–related genes were reduced in the mitochondrial FAO–inhibited fish, including proteolysis in ubiquitin-proteasome, peptide hydrolysis, and AA breakdown, which likely caused the reduction in serum AAs and the increase in muscle AAs. Growing evidence supports the notion that the general control nonderepressible 2 (GCN2) pathway also plays a primary role in the regulation of protein catabolism and shapes innate and adaptive AA responses in fish (60, 61) as in mammals (62–65). Consequently, the increased protein deposition in the mitochondrial FAO–inhibited fish might also have resulted from low protein catabolism due to the suppression of the GCN2 pathway, which was characterized by lower transcriptional levels of *gcn2*, *atf4*, and *asns*. These results indicate that the protein deposition induced by mitochondrial FAO inhibition was mediated by the activation of AKT-mTOR and the inhibition of GCN2 signaling pathways. Our findings

suggest that the mitochondrial FAO–inhibited fish preferably utilize glucose instead of AA breakdown as their metabolic fuel. This contrasts with a mammalian case in which mice with Cpt1b deficiency in muscle ($Cpt1b^{m-/-}$) exhibited upregulated expressions of genes related to AA breakdown (6). Thus, the energy homeostasis remodeling pattern could differ between fish and rodents.

In summary, elevations of glucose catabolism and protein deposition, rather than protein degradation, are the primary adaptive metabolic responses to inhibition of mitochondrial FAO in fish. These responses are regulated by the AMPK/AKT-mTOR signaling pathways. Our data clearly show that mitochondrial FAO is an important process in regulating systemic energy homeostasis in fish. Moreover, the fish with inhibited mitochondrial FAO actually have high potential to utilize glucose. These results demonstrate a new potential strategy for increasing protein deposition through energy homeostasis regulation in cultured animals.

Acknowledgments

The authors' responsibilities were as follows—L-YL and Z-YD: designed research; L-YL, J-ML, L-JN, D-L Lu, YL, and QM: conducted the experiment and sample analysis; LYL, J-ML, and QM: analyzed data; L-YL and D-L Li: generated the *cpt1b* mutant zebrafish; M-LZ, L-QC: provided essential materials and technical support; L-YL and Z-YD: drafted the manuscript; Z-YD, IJL, PD, and SML: revised the manuscript; L-YL and Z-YD: had primary responsibility for final content; and all authors: read and approved the final manuscript.

References

1. Tacon AGJ, Metian M. Food matters: fish, income, and food supply—a comparative analysis. Rev Fish Sci Aquac 2017;26:1–14.
2. Attaix D, Mosoni L, Dardevet D, Combaret L, Mirand PP, Grizard J. Altered responses in skeletal muscle protein turnover during aging in anabolic and catabolic periods. Int J Biochem Cell Biol 2005;37:1962–73.
3. Lobley GE. Protein turnover – what does it mean for animal production? Can J Anim Sci 2003;83:327–40.
4. Gale SM, Castracane VD, Mantzoros CS. Energy homeostasis, obesity and eating disorders: recent advances in endocrinology. J Nutr 2004;134:295–8.
5. Murphy KG, Bloom SR. Gut hormones and the regulation of energy homeostasis. Nature 2006;444:854–9.
6. Wicks SE, Vandanmagsar B, Haynie KR, Fuller SE, Warfel JD, Stephens JM, Wang M, Han X, Zhang J, Noland RC, et al. Impaired mitochondrial fat oxidation induces adaptive remodeling of muscle metabolism. Proc Natl Acad Sci U S A 2015;112:E3300–E9.
7. Lee J, Choi J, Selen Alpergin ES, Zhao L, Hartung T, Scafidi S, Riddle RC, Wolfgang M. Loss of hepatic mitochondrial long-chain fatty acid oxidation confers resistance to diet-induced obesity and glucose intolerance. Cell Rep 2017;20:655–67.
8. Morrow RM, Picard M, Derbeneva O, Leipzig J, McManus MJ, Gouspillou G, Barbat-Artigas S, Dos SC, Hepple RT, Murdock DG. Mitochondrial energy deficiency leads to hyperproliferation of skeletal muscle mitochondria and enhanced insulin sensitivity. Proc Natl Acad Sci U S A 2017;114:2705–10.
9. Tavecchio M, Lisanti S, Bennett MJ, Languino LR, Altieri DC. Deletion of cyclophilin D impairs β-oxidation and promotes glucose metabolism. Sci Rep 2015;5:1–11.
10. Rajeev SP, Cuthbertson DJ, Wilding JPH. Energy balance and metabolic changes with sodium-glucose co-transporter 2 inhibition. Diabetes Obes Metab 2016;18:125–34.
11. Chambers KT, Leone TC, Sambandam N, Kovacs A, Wagg CS, Lopaschuk GD, Finck BN, Kelly DP. Chronic inhibition of pyruvate dehydrogenase in heart triggers an adaptive metabolic response. J Biol Chem 2011;286:11155–62.
12. Scott D. Reduced skeletal muscle mass and lifestyle. In: Walrand S , editor. Nutrition and skeletal muscle. London: Academic Press; 2019. pp. 17–33.
13. Johnston IA, Bower NI, Macqueen DJ. Growth and the regulation of myotomal muscle mass in teleost fish. J Exp Biol 2011;214:1617–28.
14. Fry JP, Mailloux NA, Love DC, Milli MC, Ling C. Feed conversion efficiency in aquaculture: do we measure it correctly? Environ Res Lett 2018;13:024017.
15. Cowey CB. Intermediary metabolism in fish with reference to output of end products of nitrogen and phosphorus. Water Sci Technol 1995;31:21–8.
16. Polakof S, Panserat S, Soengas JL, Moon TW. Glucose metabolism in fish: a review. J Comp Physiol B 2012;182:1015–45.
17. Li LY, Limbu SM, Ma Q, Chen LQ, Zhang ML, Du ZY. The metabolic regulation of dietary L-carnitine in aquaculture nutrition: present status and future research strategies. Rev Aquacult 2019;11:1228–57.
18. Liu CZ, He AY, Ning LJ, Luo Y, Li DL, Zhang ML, Chen LQ, Du ZY. Leptin selectively regulates nutrients metabolism in Nile tilapia fed on high carbohydrate or high fat diet. Front Endocrinol[Internet] 2018;9. doi:10.3389/fendo.2018.00574.
19. Prisingkorn W, Prathomya P, Jakovlić I, Liu H, Zhao YH, Wang WM. Transcriptomics, metabolomics and histology indicate that high-carbohydrate diet negatively affects the liver health of blunt snout bream (*Megalobrama amblycephala*). BMC Genomics[Internet] 2017;18:856. doi:10.1186/s12864-017-4246-9.
20. Li JM, Li LY, Qin X, Ning LJ, Lu DL, Li DL, Zhang ML, Wang X, Du ZY. Systemic regulation of L-carnitine in nutritional metabolism in zebrafish, *Danio rerio*. Sci Rep 2017;7:1–13.
21. Ning LJ, He AY, Li JM, Lu DL, Jiao JG, Li LY, Li DL, Zhang ML, Chen LQ, Du ZY. Mechanisms and metabolic regulation of PPARα activation in Nile tilapia (*Oreochromis niloticus*). Biochim Biophys Acta Mol Cell Biol Lipids 2016;1861:1036–48.
22. Li JM, Li LY, Qin X, Degrace P, Demizieux L, Limbu SM, Wang X, Zhang MLX, Li DL, Du ZY. Inhibited carnitine synthesis causes systemic alteration of nutrient metabolism in zebrafish. Front Physiol 2018;9:1–12.
23. Karanth S, Zinkhan EK, Hill JT, Yost HJ, Schlegel A. FOXN3 regulates hepatic glucose utilization. Cell Rep 2016;15:2745–55.
24. Peng X, Shang G, Wang W, Chen X, Lou Q, Zhai G, Li D, Du Z, Ye Y, Jin X, et al. Fatty acid oxidation in zebrafish adipose tissue is promoted by $1\alpha,25(OH)_2D_3$. Cell Rep 2017;19:1444–55.
25. Liepinsh E, Vilskersts R, Loca D, Kirjanova O, Pugovichs O, Kalvinsh I, Dambrova M. Mildronate, an inhibitor of carnitine biosynthesis, induces an increase in gamma-butyrobetaine contents and cardioprotection in isolated rat heart infarction. J Cardiovasc Pharmacol 2006;48:314–9.
26. Liepinsh E, Vilskersts R, Zvejniece L, Svalbe B, Skapare E, Kuka J, Cirule H, Grinberga S, Kalvins I, Dambrova M. Protective effects of mildronate in an experimental model of type 2 diabetes in Goto-Kakizaki rats. Br J Pharmacol 2009;157:1549–56.
27. Lu DL, Ma Q, Wang J, Li LY, Han SL, Limbu SM, Li DL, Chen LQ, Zhang ML, Du ZY. Fasting enhances cold resistance in fish through stimulating lipid catabolism and autophagy. J Physiol 2019;597:1585–603.
28. Yang BY, Zhai G, Gong YL, Su JZ, Peng XY, Shang GH, Han D, Jin JY, Liu HK, Du ZY. Different physiological roles of insulin receptors in mediating nutrient metabolism in zebrafish. Am J Physiol Endocrinol Metab 2018;315:E38–51.
29. Lambert P, Dehnel PA. Seasonal variations in biochemical composition during the reproductive cycle of the intertidal gastropod *Thais lamellosa* Gmelin (*Gastropoda, Prosobranchia*). Can J Zool 1974;52:305–18.
30. Sakamoto A, Moldawer LL, Palombo JD, Desai SP, Bistrian BR, Blackburn GL. Alterations in tyrosine and protein kinetics produced by injury and branched chain amino acid administration in rats. Clin Sci 1983;64:321–31.
31. Shurubor YI, D'Aurelio M, Clark-Matott J, Isakova EP, Deryabina YI, Beal MF, Ajl C, Krasnikov BF. Determination of coenzyme A and acetyl-coenzyme A in biological samples using HPLC with UV detection. Molecules 2017;22:1–13.
32. Eames SC, Philipson LH, Prince VE, Kinkel MD. Blood sugar measurement in zebrafish reveals dynamics of glucose homeostasis. Zebrafish 2010;7:205–13.

33. Plas C, Forest N, Pringault E, Menuelle P. Contribution of glucose and gluconeogenic substrates to insulin-stimulated glycogen synthesis in cultured fetal hepatocytes. J Cell Physiol 1982;113:475–80.
34. Challiss RA, Espinal J, Newsholme EA. Insulin sensitivity of rates of glycolysis and glycogen synthesis in soleus, stripped soleus, epitrochlearis, and hemi-diaphragm muscles isolated from sedentary rats. Biosci Rep 1983;3:675–9.
35. Espinal J, Challiss RAJ, Newsholme EA. Effect of adenosine deaminase and an adenosine analogue on insulin sensitivity in soleus muscle of the rat. FEBS Lett 1983;158:103–6.
36. Olga F, Antoni I, Jaume FB, Marta B, Miguel MP, Planas JV, Josefina B. Tracing metabolic routes of dietary carbohydrate and protein in rainbow trout (*Oncorhynchus mykiss*) using stable isotopes ([^{13}C]starch and [^{15}N]protein): effects of gelatinisation of starches and sustained swimming. Br J Nutr 2012;107:834–44.
37. Ma Q, Li LY, Le JY, Lu DL, Qiao F, Zhang ML, Du ZY, Li DL. Dietary microencapsulated oil improves immune function and intestinal health in Nile tilapia fed with high-fat diet. Aquaculture 2018;496: 19–29.
38. Luo H, Jiang M, Lian G, Liu Q, Shi M, Li TY, Song L, Ye J, He Y, Yao L. AIDA selectively mediates downregulation of fat synthesis enzymes by ERAD to retard intestinal fat absorption and prevent obesity. Cell Metab 2018;27:843–53.
39. Betancor MB, Sprague M, Sayanova O, Usher S, Campbell PJ, Napier JA, Caballero MJ, Tocher DR. Evaluation of a high-EPA oil from transgenic *Camelina sativa* in feeds for Atlantic salmon (*Salmo salar* L.): effects on tissue fatty acid composition, histology and gene expression. Aquaculture 2015;444:1–12.
40. Osama AA, Lopaschuk GD. Role of CoA and acetyl-CoA in regulating cardiac fatty acid and glucose oxidation. Biochem Soc Trans 2014;42:1043–51.
41. Lei S, Tu BP. Acetyl-CoA and the regulation of metabolism: mechanisms and consequences. Curr Opin Cell Biol 2015;33:125–31.
42. Altamimi TR, Thomas PD, Darwesh AM, Fillmore N, Mahmoud MU, Zhang L, Gupta A, Al Batran R, Seubert JM, Lopaschuk GD. Cytosolic carnitine acetyltransferase as a source of cytosolic acetyl-CoA: a possible mechanism for regulation of cardiac energy metabolism. Biochem J 2018;475:959–76.
43. Wu L, Zhang L, Li B, Jiang H, Duan Y, Xie Z, Shuai L, Li J, Li J. AMP-activated protein kinase (AMPK) regulates energy metabolism through modulating thermogenesis in adipose tissue. Front Physiol 2018;9: 1–23.
44. Grahame HD, Ross FA, Hawley SA. AMPK: a nutrient and energy sensor that maintains energy homeostasis. Nat Rev Mol Cell Biol 2012;13:251–62.
45. Hardie DG. AMPK: positive and negative regulation, and its role in whole-body energy homeostasis. Curr Opin Cell Biol 2015;33:1–7.
46. Lin SC, Hardie DG. AMPK: sensing glucose as well as cellular energy status. Cell Metab 2017;27:299–313.
47. Koves TR, Ussher JR, Noland RC, Slentz D, Mosedale M, Ilkayeva O, Bain J, Stevens R, Dyck JRB, Newgard CB. Mitochondrial overload and incomplete fatty acid oxidation contribute to skeletal muscle insulin resistance. Cell Metab 2008;7:45–56.
48. Polakof S, Panserat S, Craig PM, Martyres DJ, Elisabeth PJ, Sharareh S, Stéphane AB, Moon TW. The metabolic consequences of hepatic AMP-kinase phosphorylation in rainbow trout. PLoS One 2011;6:e20228.
49. Magnoni LJ, Vraskou Y, Palstra AP, Planas JV. AMP-activated protein kinase plays an important evolutionary conserved role in the regulation of glucose metabolism in fish skeletal muscle cells. PLoS One 2012;7:e31219.
50. Xu C, Li XF, Tian HY, Shi HJ, Zhang DD, Abasubong KP, Liu WB. Metformin improves the glucose homeostasis of Wuchang bream fed high-carbohydrate diets: a dynamic study. Endocr Connect 2019;8:182–94.
51. Otero-Rodiño C, Velasco C, Álvarez-Otero R, López-Patiño MA, MãGuez JM, Soengas JL. Changes in the levels and phosphorylation status of Akt, AMPK, CREB, and FoxO1 in hypothalamus of rainbow trout under conditions of enhanced glucosensing activity. J Exp Biol 2017;220:4410–7.
52. Jin J, Mãdale F, Kamalam BS, Aguirre P, Vãron V, Panserat S. Comparison of glucose and lipid metabolic gene expressions between fat and lean lines of rainbow trout after a glucose load. PLoS One 2014;9:e105548.
53. Vandanmagsar B, Warfel J, Wicks S, Ghosh S, Salbaum JM, Burk D, Dubuisson O, Mendoza T, Zhang J, Noland R. Impaired mitochondrial fat oxidation induces FGF21 in muscle. Cell Rep 2016;15:1686–99.
54. Delaere F, Magnan C, Mithieux G. Hypothalamic integration of portal glucose signals and control of food intake and insulin sensitivity. Diabetes Metab 2010;36:257–62.
55. Carmen N, Valverde AM, Manuel B. Role of insulin receptor in the regulation of glucose uptake in neonatal hepatocytes. Endocrinology 2006;147:3709–18.
56. Zhan T, Digel M, Küch E-M, Stremmel W, Joachim F. Silybin and dehydrosilybin decrease glucose uptake by inhibiting GLUT proteins. J Cell Biochem 2015;112:849–59.
57. Penumathsa S, Thirunavukkarasu M, Zhan L, Maulik G, Menon V, Bagchi D, Maulik N. Resveratrol enhances GLUT-4 translocation to the caveolar lipid raft fractions through AMPK/Akt/eNOS signalling pathway in diabetic myocardium. J Cell Mol Med 2010;14:2350–61.
58. Seiliez I, Panserat S, Skiba-Cassy S, Polakof S. Effect of acute and chronic insulin administrations on major factors involved in the control of muscle protein turnover in rainbow trout (*Oncorhynchus mykiss*). Gen Comp Endocrinol 2011;172:363–70.
59. Saxton RA, Sabatini DM. mTOR signaling in growth, metabolism, and disease. Cell 2017;168:960–76.
60. Zhen W, Mai K, Wei X, Zhang Y, Liu Y, Ai Q. Dietary methionine level influences growth and lipid metabolism via GCN2 pathway in cobia (*Rachycentron canadum*). Aquaculture 2016;454:148–56.
61. Jiang H, Bian F, Zhou H, Wang X, Wang K, Mai K, He G, Jiang H, Bian F, Zhou H. Nutrient sensing and metabolic changes after methionine deprivation in primary muscle cells of turbot (*Scophthalmus maximus* L.). J Nutr Biochem 2017;50:74–82.
62. Marine L, Stephane P, Plagnes-Juan E, Karine D, Iban S, Sandrine S-C. L-leucine, L-methionine, and L-lysine are involved in the regulation of intermediary metabolism-related gene expression in rainbow trout hepatocytes. J Nutr 2011;141:75–80.
63. Kilberg MS, Pan YX, Chen H, Leungpineda V. Nutritional control of gene expression: how mammalian cells respond to amino acid limitation. Annu Rev Nutr 2005;25:59–85.
64. Jordan G, Eylul H, Mitchell JR. Amino acid sensing in dietary-restriction-mediated longevity: roles of signal-transducing kinases GCN2 and TOR. Biochem J 2013;449:1–10.
65. Chaveroux C, Lambert-Langlais S, Cherasse Y, Averous J, Parry L, Carraro V, Jousse C, Maurin AC, Bruhat A, Fafournoux P. Molecular mechanisms involved in the adaptation to amino acid limitation in mammals. Biochimie 2010;92:736–45.